Global and Planetary Change 184 (2020) 103047

Contents lists available at ScienceDirect

Global and Planetary Change

journal homepage: www.elsevier.com/locate/gloplacha

Research article

Changes in surface hydrography at the western tropical Atlantic during the Younger Dryas

I.M. Venancio[a,*], M.H. Shimizu[a], T.P. Santos[b], D.O. Lessa[b], R.C. Portilho-Ramos[c], C.M. Chiessi[d], S. Crivellari[e], S. Mulitza[c], H. Kuhnert[c], R. Tiedemann[f], M. Vahlenkamp[c], T. Bickert[c], G. Sampaio[a], A.L.S. Albuquerque[b], S. Veiga[a], P. Nobre[a], C. Nobre[g]

[a] Center for Weather Forecasting and Climate Studies (CPTEC), National Institute for Space Research (INPE), Cachoeira Paulista, Brazil
[b] Programa de Geociências (Geoquímica), Universidade Federal Fluminense, Niterói, Brazil
[c] MARUM-Center for Marine Environmental Sciences, University of Bremen, Bremen, Germany
[d] School of Arts, Sciences and Humanities, University of São Paulo, São Paulo, Brazil
[e] Institute of Geosciences, University of São Paulo, São Paulo, Brazil
[f] Alfred Wegener Institute for Polar and Marine Research, Bremerhaven, Germany
[g] Institute for Advanced Studies, University of São Paulo, São Paulo, Brazil

A B S T R A C T

During the Younger Dryas (YD), paleoceanographic proxies indicate a weakening of the Atlantic Meridional Overturning Circulation (AMOC) resulting in a widespread surface cooling of the North Atlantic and a southward displacement of the Intertropical Convergence Zone (ITCZ). In the western tropical Atlantic, competing ocean and atmospheric processes may result in contrasting surface hydrography scenarios north and south of the equator during the YD. Based on new and compiled data, we provide an up-to-date model-data comparison of changes in western tropical Atlantic surface hydrography during the YD. We show that both transient model simulations and proxy results indicate warming of sea surface temperatures (SST) in the western tropical South Atlantic, but disagree for the SST in the western tropical North Atlantic. Proxies also reveal a complex spatial pattern in surface salinity in the western tropical Atlantic, while a broad negative anomaly is observed in the model output. By comparing planktonic foraminiferal Ba/Ca records from different records in the western tropical Atlantic we constrain ITCZ shifts from the YD to the early Holocene. Based on the Ba/Ca records, the ITCZ reached its southernmost position between 13 and 11.8 ka and started to move northward reaching its northernmost position between 10.8 and 9.7 ka.

1. Introduction

Over the course of the last deglaciation, the warming trend in the North Atlantic was discontinuous due to the occurrence of abrupt cooling events such as the Younger Dryas (YD) (12.9–11.6 ka) (Carlson, 2013). Several mechanisms such as reduced solar activity (Renssen et al., 2000) and an extraterrestrial impact (Firestone et al., 2007) may have caused the YD and promoted its global climate signal (Renssen et al., 2015). However, the most accepted cause of the YD is the drainage of Lake Agassiz, which increased freshwater discharge to the North Atlantic and, consequently, abruptly reduced the strength of the Atlantic Meridional Overturning Circulation (AMOC) (Johnson and McClure, 1976; Rooth, 1982; Broecker et al., 1985).

During the YD, Greenland ice cores (NGRIP members, 2004) and sea surface temperature (SST) records from the northeastern North Atlantic (Bard et al., 2000) reveal an abrupt cooling. In the western tropical Atlantic, the scenario is more complex (Carlson, 2013). SST records show a warming of the Caribbean, Tobago Basin and off northeastern Brazil (Schmidt et al., 2004; Rühlemann et al., 1999; Weldeab et al., 2006), while cooling is indicated at Barbados, Cariaco and Guiana Basins (Guilderson et al., 2001; Lea et al., 2003; Rama-Corredor et al., 2015).

Paleoclimate proxies from the western tropical Atlantic provide evidence for a southward shift of the Intertropical Convergence Zone (ITCZ) during the YD (Haug et al., 2001; Wang et al., 2004; Portilho-Ramos et al., 2017; Bouimetarhan et al., 2018; Reißig et al., 2019). This should have lead to an increase in sea surface salinity (SSS) over the western tropical North Atlantic and a decrease in the western tropical South Atlantic, as pointed out by Wan et al. (2010). However, positive SSS anomalies have been reconstructed for the northern and southern western tropical Atlantic during the YD (Schmidt et al., 2004; Weldeab et al., 2006; Hoffmann et al., 2014). Thus, additional factors forcing the changes in surface hydrography (SST and SSS) in the western tropical Atlantic are required during the YD.

Here we investigate changes in surface hydrography during the YD in the western tropical Atlantic. Specifically, our goals are to: (1)

* Corresponding author.
E-mail address: igor.venancio@inpe.br (I.M. Venancio).

https://doi.org/10.1016/j.gloplacha.2019.103047
Received 24 April 2019; Received in revised form 20 September 2019; Accepted 24 September 2019
Available online 16 October 2019

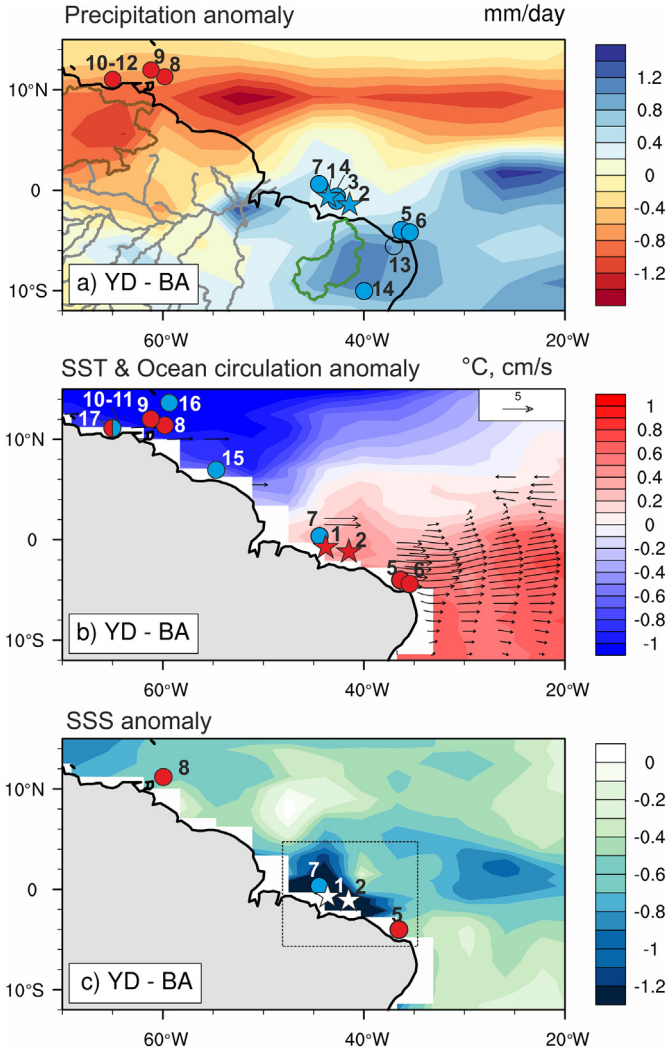

Fig. 1. TraCE-21 ka (Liu et al., 2009) precipitation, temperature and salinity anomalies during the Younger Dryas (12.9–11.6 ka) relative to the Bølling–Allerød (14.7–13 ka) (YD-BA) together with the location of the studied cores (stars: GL-1248, marked as 1 and GeoB16202–2, marked as 2), as well as other tropical records (see Table S1 for identification of each record). (a) YD-BA precipitation anomaly from TraCE-21 ka (color-scale) and proxy information (circles). Information regarding precipitation changes during the YD (wetter – blue, drier – red and no change – no fill) derived from proxies is displayed. The lines in the continent represent the tributaries (or catchments) of the Amazon (grey), Parnaíba (green) and Orinoco Rivers (brown). (b) YD-BA sea surface temperature (SST) (color-scale) and surface ocean circulation (arrows) anomalies from TraCE-21 ka and proxy information (circles). Information regarding SST changes during the YD (warmer – red and colder – blue) derived from proxies is shown. (c) YD-BA sea surface salinity (SSS) (color-scale) anomaly from TraCE-21 ka and proxy ($\delta^{18}O_{sw\text{-}ivc}$) information (circles). Information regarding SSS changes during the YD (saltier – red, fresher – blue and no significant change – white) derived from proxies is shown. The rectangle with dashed lines marks the area of major decrease in SSS. (For interpretation of the references to color in this figure legend, the reader is referred to the web version of this article.)

provide an up-to-date compilation of surface hydrographic proxies for the YD in the western tropical Atlantic; (2) compare the proxy compilation with a state-of-the-art coupled climate model simulation for the last deglaciation using the Community Climate System Model CCSM3 (TraCE-21 ka; Liu et al., 2009; He, 2011); (3) investigate the associated ocean-atmosphere processes; and (4) reconstruct ITCZ shifts. We present new records of surface hydrographic changes during the YD based on $\delta^{18}O$, Mg/Ca and Ba/Ca from planktonic foraminifera species *Globigerinoides ruber* for cores GL-1248 and GeoB16202-2 collected in the western tropical South Atlantic.

2. Study area

Cores GL-1248 (0°55.2′S, 43°24.1′W, 2264 m water depth) and GeoB16202-2 (1°54.50′ S, 41°35.50′ W, 2248 m water depth) were collected from the continental slope off northeastern Brazil (Fig. 1). Upper ocean circulation in the western South Atlantic is dominated by the northward-flowing North Brazil Current (NBC), which originates from the bifurcation of the South Equatorial Current (SEC) around 10°S (Peterson and Stramma, 1991; Stramma and England, 1999). In the upper-ocean (< 100 m), the NBC transports Tropical Water (TW), which is a warm (> 20 °C) and saline (> 36) water mass (Stramma and England, 1999).

Seasonal changes in the trade wind system drive the variability of the NBC transport (Stramma et al., 1995). During austral summer and fall the ITCZ relocates southward, and the northeast (NE) trade winds strengthen (Hastenrath and Merle, 1987). This shifts the SEC bifurcation northward and weakens the NBC (Rodrigues et al., 2007). At the same time rainfall over northeastern Brazil increases, peaking from March until April. During austral winter and spring, the southeast (SE) trade winds strengthen and the ITCZ mean position is displaced northward, consequently decreasing the precipitation over northeastern Brazil (Hastenrath and Merle, 1987).

3. Material and Methods

We analyzed the uppermost portions of cores GL-1248 (upper 1.6 m) and GeoB16202-2 (upper 3.0 m). The complete age models of cores GL-1248 and GeoB16202-2 were previously published in Venancio et al. (2018) and Mulitza et al. (2017), respectively. Radiocarbon samples containing tests of *G. ruber* and *Trilobatus sacculifer* were handpicked from the fraction larger than 150 µm. Samples from core GL-1248 were analyzed at Beta Analytic Radiocarbon Dating Laboratory, while samples from core GeoB16202-2 were analyzed at the Poznań Radiocarbon Laboratory. Radiocarbon ages for both cores were calibrated with the IntCal13 calibration curve (Reimer et al., 2013) with a reservoir age of 400 ± 200 years (2σ) and no additional local reservoir effect (ΔR = 0). The age model of core GL-1248 was constructed using linear interpolation with the software clam 2.2 (Blaauw, 2010), while the software BACON version 2.2 (Blaauw and Christeny, 2011) was used for constructing the age model of core GeoB16202-2. Some of the radiocarbon ages of both cores suggest calibrated ages within the YD chronozone.

Ten tests of *G. ruber* (white) (250–355 µm) from core GL-1248 and five to ten tests of *G. ruber* (white) (350–500 µm) from core GeoB16202–2 were analyzed for oxygen stable isotopes ($\delta^{18}O$). All tests were handpicked under a binocular microscope. Oxygen isotope analyses were performed with a Finnigan MAT 252 mass spectrometer equipped with an automatic carbonate preparation device at MARUM, University of Bremen (Germany). Isotopic results were calibrated relative to the Vienna Pee Dee Belemnite (VPDB) using the NBS19. The standard deviation of the laboratory standard was lower than 0.07‰ for the measuring period. These results were previously reported in Venancio et al. (2018).

Mg/Ca and Ba/Ca were analyzed in planktonic foraminifera *G. ruber* (white). For core GL-1248, Mg/Ca and Ba/Ca analyses were performed on samples comprising 30 shells of *G. ruber* (white, 250–300 µm). For core GeoB16202–2, Mg/Ca analyses were performed on samples with 10–30 shells of *G. ruber* (white) (350–500 µm) (Vahlenkamp, 2013). Samples were gently crushed and cleaned following the procedure described by Barker et al. (2003). Before dilution, samples were centrifuged for 10 min to exclude any remaining insoluble particles from the analyses (Groeneveld and Chiessi, 2011). The diluted solutions were analyzed with an ICP-OES Agilent Technologies 700 Series with an autosampler (ASX-520 Cetac) and a micro-nebulizer at MARUM. Each

Mg/Ca and Ba/Ca value is averaged from three replicate runs. After every five samples one of two laboratory standards was measured to estimate the external reproducibility. Means ± 1 SD were 5.165 ± 0.024 mmol/mol for Mg/Ca and 14.37 ± 0.14 µmol/mol for Ba/Ca for standard 1 (n = 96), and 3.294 ± 0.012 mmol/mol for Mg/Ca and 3.04 ± 0.10 µmol/mol for Ba/Ca for standard 2 (n = 67). Elements were measured at the following spectral lines: Mg (279.553 nm), Ca (315.887 nm), Ba (455.403 nm), Al (167.019 nm), Fe (238.204 nm), and Mn (257.610 nm). The calibrated concentration range for Ca was 5–80 ppm. Two sets of calibration solutions were used on different portions of the core, with Mg/Ca and Ba/Ca close to those of the two laboratory standards. Each set comprised four or five different dilutions, plus one blank. Ba/Ca outliers (values higher than Quartile3 + 1.5 x Interquartile Range) were removed (Fig. S1) and represent 6.5% of the dataset. Only samples with Al/Ca < 0.5 mmol/mol were used. Contamination was also monitored by analyzing the Fe/Ca and Mn/Ca ratios. The Fe/Ca and Mn/Ca ratios in some of our samples were higher than the 0.1 mmol/mol cutoff proposed by Barker et al. (2003). However, correlations between Ba/Ca and Mg/Ca with Fe/Ca and Mn/Ca were insignificant (R^2 < 0.1, p > > 0.1) (Fig. S2). This suggests that our analyses were not affected by the presence of mineral phases rich in Fe and Mn. The Mg/Ca results were converted to temperature values using the Mg/Ca-temperature equation of Anand et al. (2003).

The $\delta^{18}O$ of seawater ($\delta^{18}O_{sw}$) was estimated using Mg/Ca and $\delta^{18}O$ from *G. ruber* (white) and by applying the paleotemperature equation of Mulitza et al. (2003) together with the obtained Mg/Ca-SST. A conversion constant of 0.27‰ was applied to convert the values from VPDB to Vienna Standard Mean Ocean Water (VSMOW) (Hut, 1987). The effect of changes in global sea level was subtracted from the $\delta^{18}O_{sw}$ by considering the sea level reconstruction of Grant et al. (2012) and a glacial $\delta^{18}O$ increase of 0.008‰ m^{-1} sea level lowering (Schrag et al., 2002). $\delta^{18}O_{sw}$ estimation takes into account an uncertainty of 1 °C for the Mg/Ca-SST equation from Anand et al. (2003), which is equivalent to 0.2‰ $\delta^{18}O$ change (Mulitza et al., 2003) and an analytical error for $\delta^{18}O$ of 0.07‰. Hence, the propagated error estimated for the $\delta^{18}O_{sw}$ was ± 0.21‰.

4. Results

For core GL-1248, the $\delta^{18}O$ values of *G. ruber* (white) are between −1.88 and − 0.84‰, and Mg/Ca values range from 3.87 to 5.01 mmol/mol (Fig. S3). Estimates of SST based on Mg/Ca values of *G. ruber* (white) are between 25.8 and 28.7 °C (Fig. S3). Mg/Ca-SST exhibit only a minor increase from 26.5 to 27.6 °C during the YD. The $\delta^{18}O_{sw\text{-}ivc}$ values vary between 1.10 and 1.82‰, with high values during the mid-Holocene (1.82‰) (Fig. S3). Ba/Ca of *G. ruber* (white) values range from 1.14 to 3.20 µmol/mol, increasing abruptly from 1.15 to 3.25 µmol/mol during the YD (Fig. S3). For core GeoB16202–2, the $\delta^{18}O$ values of *G. ruber* (white) are between −1.74 and − 0.70‰ and Mg/Ca values range from 3.91 to 4.99 mmol/mol (Fig. S3). Mg/Ca-SST vary from 25.9 to 28.6 °C, where an increase in Mg/Ca-SST up to 28.1 °C is present during the YD (Fig. S3). The $\delta^{18}O_{sw\text{-}ivc}$ vary from 1.28 to 1.91‰, with high values during the YD and the mid-Holocene (Fig. S3), similarly to core GL-1248.

5. Discussion

5.1. SST responses over the western tropical Atlantic during the Younger Dryas

The SST estimates from model results and proxy data indicate a warming of the western tropical South Atlantic during the YD relative to the Bølling-Allerød (BA) (Figs. 1b and 2c). Model and proxy data agree regarding the magnitude of such warming during the YD relative to the BA (YD-BA) in the western South Atlantic. TraCE-21 ka results show < 1 °C warming in the western tropical South Atlantic (Fig. 1b), which is supported by the proxy results (Weldeab et al., 2006; Jaeschke et al., 2007; this study) that show increases in SST between 0.2 and 1.0 °C for the YD-BA. This agreement between model and proxy data in the sign of SST change during the YD, however, is not observed for the western tropical North Atlantic (Fig. 1b). In addition, although some records display a cooling (Guilderson et al., 2001; Lea et al., 2003; Nace et al., 2014; Rama-Corredor et al., 2015), which is also revealed by the TraCE-21 ka results (Liu et al., 2009), other records suggest a warming during the YD-BA (Rühlemann et al., 1999; Schmidt et al., 2012; Hoffmann et al., 2014). The incongruence between model and proxy SST for the western tropical North Atlantic may be a consequence of local oceanic changes and/or proxy sensitivity, as described below.

Wan et al. (2009) using model simulations suggested that the complex SST pattern during the YD in the tropics is the result of competing oceanographic and atmospheric processes. The authors show that if SST changes are only attributed to ocean circulation changes, during the YD the weakened AMOC produces a surface warming in the entire tropical Atlantic basin. This surface warming originates in the subsurface of the ocean and is caused by the weakening of the western boundary currents (Chang et al., 2008). In another model experiment, with no change in ocean circulation during the YD, Wan et al. (2009) observed a surface cooling in the tropical Atlantic basin due to a series of ocean-atmosphere feedback mechanisms, for example the wind-evaporation-SST (WES) feedback (Xie and Philander, 1994; Chang et al., 1997), that intensified the evaporative cooling in the region. Extensive ice cover in the northern high latitudes cools and dries the atmosphere above the sea surface initiating a cooling of the northern high- and mid-latitudes through advection, and then the WES feedback provides a further progression of the cold SST signal to low latitudes. The resulted meridional SST gradient induces a southward shift of the ITCZ and positive ocean-atmosphere feedbacks amplify and maintain this ITCZ displacement. Summarizing, WES feedback enhances the propagation of the high-latitude cooling to the TNA and is responsible for the southward ITCZ shift, as for the development of a cross-equatorial SST gradient with a negative SST anomaly in the TNA and positive anomaly in the TSA (Chiang and Bitz, 2005; Mahajan et al., 2011). Thus, as suggested by Wan et al. (2009) the SST proxy signal (warming or cooling) depends on whether the temperature change at the site is dominated by atmospheric or oceanic processes. We suggest that in the TNA it is possible that surface cooling produced by reduced cross-equatorial ocean heat transport and the WES feedback counterbalanced an increase in SST triggered by a change in heat advection in the subsurface (Schmidt et al., 2012). However, in the TSA such counterbalance effect is probably not occurring, as evidenced by the similar SST patterns between the records. The SST response in the TSA during the YD is probably linked to the heat accumulation due to reduced cross-equatorial ocean heat transport and by a weakening of the NBC (Arz et al., 1999; Chang et al., 2008; Zhang et al., 2015).

In the TNA, the mismatch between proxy results might also be due to proxy sensitivity or other factors that influence the different proxies. Crivellari et al. (2019) point out that the negative anomalies during millennial-scale events shown by the alkenone-based record from MD03–2616 (Rama-Corredor et al., 2015) are probably the result of non-thermal physiological effects on the alkenone producers related to the presence of the Amazon River plume. This is supported by the fact that northern records (M-78/1–235-1 and M35003–4), which are less (or not) influenced by the plume of the Amazon River, show positive SST anomalies during the YD (Rühlemann et al., 1999; Hoffmann et al., 2014). Although Amazon freshwater may reach the Caribbean under modern conditions (Muller-Karger et al., 1988), in a YD scenario of southward ITCZ migration, strong NE trade winds and weak NBC, these northern records (M-78/1–235-1 and M35003–4) were probably less (or not) influenced by the Amazon plume. In another TNA site, Guilderson et al. (2001) suggested a cooling based on the $\delta^{18}O$ data from Barbados corals, but this may be overestimated since increased

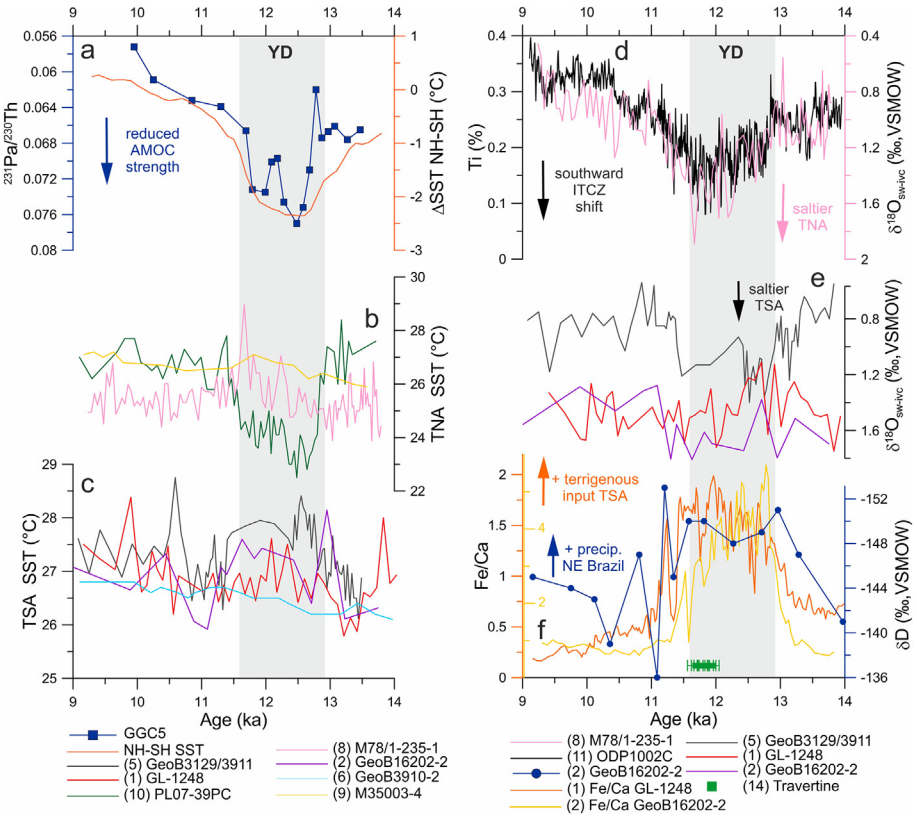

Fig. 2. Paleoceanographic proxies covering the final portion of the last deglaciation and the early Holocene. (a) ^{231}Pa/^{230}Th record from core OCE326-GGC5 (McManus et al., 2004) (blue line and squares) and reconstruction of hemispheric sea surface temperature difference (Shakun et al., 2012) (orange line). (b) Sea surface temperature (SST) records from cores located in the western tropical North Atlantic (TNA). SST records from cores PL07-39PC (Lea et al., 2003; ID: 10) (green line), M78/1-235-1 (Hoffmann et al., 2014; ID: 8) (pink line) and M35003-4 (Rühlemann et al., 1999; ID: 9) (yellow line). (c) SST records from cores located in the western tropical South Atlantic (TSA). SST records from cores GeoB3910–2 (Jaeschke et al., 2007; ID: 6) (light blue line), GeoB3129-1/3911-3 (Weldeab et al., 2006; ID: 5) (grey line), GeoB16202-2 (this study; ID: 2) (purple line) and GL-1248 (this study; ID: 1) (red line). Panels (b) and (c) do not show all records displayed in Fig. 1b, since not all records were available in data publishers. (d) Titanium content in sediments of the Cariaco Basin (Haug et al., 2001; ID: 11) (black line) and ice volume corrected $\delta^{18}O$ of seawater ($\delta^{18}O_{sw-ivc}$) record from core M78/1–235-1 (Hoffmann et al., 2014; ID: 8) (pink line) located in the TNA. (e) $\delta^{18}O_{sw-ivc}$ from cores located in the TSA, GeoB3129/3911 (Weldeab et al., 2006; ID: 5) (grey line), GeoB16202–2 (this study; ID: 2) (purple line) and GL-1248 (this study; ID: 1) (red line). (f) Fe/Ca (a proxy linked to precipitation changes) ratios from cores GL-1248 (this study; ID: 1) (orange) and GeoB16202–2 (Mulitza et al., 2017; ID: 2) (yellow), travertine growth from northeastern Brazil (Wang et al., 2004; ID: 14) (green squares) and ice volume corrected δD of terrestrial plant wax from core GeoB16202–2 (Mulitza et al., 2017; ID: 2) (blue line and dots). Grey bar marks the Younger Dryas. (For interpretation of the references to color in this figure legend, the reader is referred to the web version of this article.)

coral $\delta^{18}O$ may as well be produced by enhanced salinity. In the Cariaco Basin, the negative SST anomaly described by Lea et al. (2003) can be a local signal caused by enhanced upwelling during the YD due to strong NE trade winds and consequently increased Ekman transport. Finally, the low sedimentation rate (i.e., 3 cm/kyr) of the composite core CDH-86/GGC-81/BC-82 (Nace et al., 2014) prevents a detailed investigation of a YD signal. The above reasons might explain the different signs of the proxy-based SST anomalies in the TNA during the YD. Since Wan et al. (2009) focused solely on the investigation of the physical processes, our evaluations regarding the proxies signals contribute significantly to the understanding of the SST pattern in the western tropical Atlantic during the YD.

Furthermore, we show that the most representative proxies in the TNA show a positive SST anomaly in the TNA, which does not match the TraCE-21 ka results but is in agreement with results from other model simulations that focused on events of AMOC slowdown (Knutti et al., 2004; Kageyama et al., 2009). The cooling in the TNA revealed by the TraCE-21 ka simulations can be associated to bipolar seesaw response, manifested even in low latitudes of the North Atlantic, or to the WES feedback and its connection with ITCZ dynamics, since this model may overestimate climate variability linked to the ITCZ over the tropical Atlantic (Liu et al., 2009).

5.2. Model-data comparison of SSS anomalies over the western tropical Atlantic

SSS anomalies ($\delta^{18}O_{sw-ivc}$) from most records indicate an increase or no clear change (Fig. 1c and 2e), while the TraCE-21 ka results (Liu et al., 2009) point towards a decrease in SSS in the western tropical Atlantic during the YD (Fig. 1c). A decrease in SSS in the western tropical South Atlantic is consistent with the presence of an atmospheric forcing, where increased precipitation over the ocean (Fig. 1a) occurs due to a southward displacement of the ITCZ during the YD (Fig. 2d; Haug et al., 2001). The increase in continental precipitation over northeastern Brazil (Fig. 1a and 2f), which is supported by speleothem $\delta^{18}O$, deuterium isotopic composition of plant waxes and palynological records (Wang et al., 2004; Mulitza et al., 2017; Bouimetarhan et al., 2018), resulted in enhanced freshwater discharge, explaining reduced SSS close to the mouths of the Amazon and Parnaíba Rivers (Fig. 1c). Although $\delta^{18}O_{sw-ivc}$ is affected by freshwater discharge and evaporation-precipitation balance the $\delta^{18}O_{sw-ivc}$ results from most cores did not capture the negative SSS anomaly during the YD displayed by the TraCE-21 ka results, with exception of CDH-86 (Nace et al., 2014). Some $\delta^{18}O_{sw-ivc}$ records show an increase in SSS in the TNA (Hoffmann et al., 2014) and TSA (Weldeab et al., 2006) during the YD. In the TSA, the increase in $\delta^{18}O_{sw-ivc}$ (or SSS) may be explained by a reduction of the cross-equatorial transport of saline waters and a weakening of the NBC, which would accumulate saline waters in this area (Weldeab et al., 2006). However, for the TNA the increase in $\delta^{18}O_{sw-ivc}$ can be related to higher wind stress and evaporation and reduced precipitation in this area (Fig. 1a; Hoffmann et al., 2014), or to a coastal upwelling of subsurface warm and saline waters (Wan et al., 2009; Schmidt et al., 2012). These responses linked to the increase of SSS are not supported by the TraCE-21 ka results (Liu et al., 2009). By comparing modern SSS values from TraCE-21 ka to modern SSS datasets (Fig. S4) we notice that TraCE-21 ka results underestimate the SSS in the study area. This indicates that this model may not provide an ideal representation of SSS for the western tropical Atlantic. Although the model results show increased convergence of winds at low levels of the atmosphere that support the increased precipitation in the TSA due to southward ITCZ migration (Fig. S5), the model may overestimate the influence of the ITCZ over the tropics (Liu et al., 2009) producing the observed SSS pattern during the YD (Fig. 1c).

Although TraCE-21 ka underestimates the SSS in the western

tropical Atlantic, we may consider an alternative explanation for the lack of a strong decrease in $\delta^{18}O_{sw\text{-}ivc}$ in most records. The $\delta^{18}O_{sw\text{-}ivc}$ records from GL-1248 and GeoB16202-2 suggest a decrease in $\delta^{18}O_{sw}$ (lower SSS) and an increase in $\delta^{18}O_{sw}$ (higher SSS), respectively, across the YD, but the changes are within error limits (< 0.21‰). Thus, neither a strong decrease nor increase in $\delta^{18}O_{sw\text{-}ivc}$ is recorded in cores GL-1248 and GeoB16202-2. A possible explanation is that the accumulation of salty waters due to a decrease in AMOC strength produces a positive SSS anomaly. Some $\delta^{18}O_{sw\text{-}ivc}$ records (GeoB 3129-1/GeoB 3911-3 and M78/1-235-1) show increases in $\delta^{18}O_{sw\text{-}ivc}$ during the YD (Fig. 1c), probably due to a larger positive SSS anomaly, linked to reduced AMOC strength, than the negative anomaly by the processes mentioned above. At the same time, other records show a decrease (CDH-86) or no clear change (GL-1248 and GeoB16202-2) in $\delta^{18}O_{sw\text{-}ivc}$ during the YD. These records are close to major rivers (Amazon and Parnaíba) that probably increased their discharge during the YD, as revealed by previous studies (i.e. Zhang et al., 2015) and the TraCE-21 ka results (Fig. S6). Thus, an increase in river runoff probably dampened the AMOC-driven SSS increase at these sites. This highlights the importance of considering local factors (i.e. river discharge) to understand the SSS spatial pattern in the western tropical Atlantic during the YD. Wan et al. (2010) discarded the changes in river discharge as a major process, but they did not have the information provided by these new $\delta^{18}O_{sw\text{-}ivc}$ records (CDH-86, Nace et al., 2014; GL-1248 and GeoB16202-2, this study).

5.3. Changes in fluvial discharge recorded by Ba/ca of planktonic foraminifera

Since Ba/Ca of seawater is incorporated into foraminiferal calcite with no dependency on temperature or salinity (Hönisch et al., 2011) and fluvial waters have higher Ba/Ca than seawater (Hall and Chan, 2004), Ba/Ca ratio can be used as a proxy for river runoff (Bahr et al., 2013; Hoffmann et al., 2014). The high Ba/Ca values of *G. ruber* from core GL-1248 reveal an enhanced fluvial freshwater discharge to the western equatorial Atlantic during the YD (Fig. 3a), probably from the Parnaíba River as suggested by sediment provenance proxies from an adjacent core (Zhang et al., 2015). Although Ba/Ca generally reflects changes in fluvial water input, it may be modified by changes in the Ba/Ca-endmember of the river water and by changes in mixed layer productivity (Bahr et al., 2013). However, as pointed out by Bahr et al. (2013) if Ba/Ca of *G. ruber* was modulated by productivity changes, it should correlate with the $\delta^{13}C$ of *G. ruber*, which is not the case for our results (Fig. S7). In addition, similarly to the findings of Bahr et al. (2013), our high Ba/Ca values occur concomitantly with low abundances of productivity-related planktonic foraminiferal species (i.e. *Globigerina bulloides*) (Fig. S8), which reinforces our interpretation that the high Ba/Ca values during the YD are indeed linked to an increase in fluvial discharge.

We are not able to exclude possible changes of the Ba/Ca-endmember, since information on the concentration of Ba^{2+} in the different tributaries of the Parnaíba River is not available. However, since the Parnaíba drainage basin is relatively small, we do not expect that major changes in the composition of the freshwater source within the basin happened from the BA to the YD. Further, high Ba/Ca values occur simultaneously with high sedimentary Fe/Ca (Fig. 2f) in core GL-1248 suggesting that the increase in Ba/Ca during the YD is more likely caused by enhanced river runoff (Fig. 3). A major increase in river runoff during the YD is in agreement with TraCE-21 ka simulations (Fig. S6), which also indicate an enhanced precipitation over parts of the drainage basins of the Amazon and Parnaíba Rivers (Fig. 3a). In addition, a peak in Fe/Ca during the YD is also evident in other cores from this region (Zhang et al., 2015; Mulitza et al., 2017; Bouimetarhan et al., 2018), supporting the hypothesis of enhanced runoff of the Parnaíba River.

The similarity between Ba/Ca recorded in *G. ruber* (white) and Fe/Ca values from core GL-1248 (Fig. S3) indicates that the high Ba/Ca values are caused by desorption of Ba^{2+} from the river suspension load, similar to what occurs in the modern Orinoco discharge area (Bahr et al., 2013). In addition, this mechanism would explain why we observe a divergence between the Ba/Ca and $\delta^{18}O_{sw\text{-}ivc}$ from core GL-1248 during the YD. Bahr et al. (2013) suggested different mixing behaviors for Ba/Ca and $\delta^{18}O_{sw\text{-}ivc}$, it is conservative for $\delta^{18}O_{sw\text{-}ivc}$ and non-linear for Ba/Ca. In this sense, Bahr et al. (2013) using samples from the western tropical Atlantic showed that high Ba/Ca ratios in foraminiferal calcite can be recorded without any change in the $\delta^{18}O$. Therefore, with

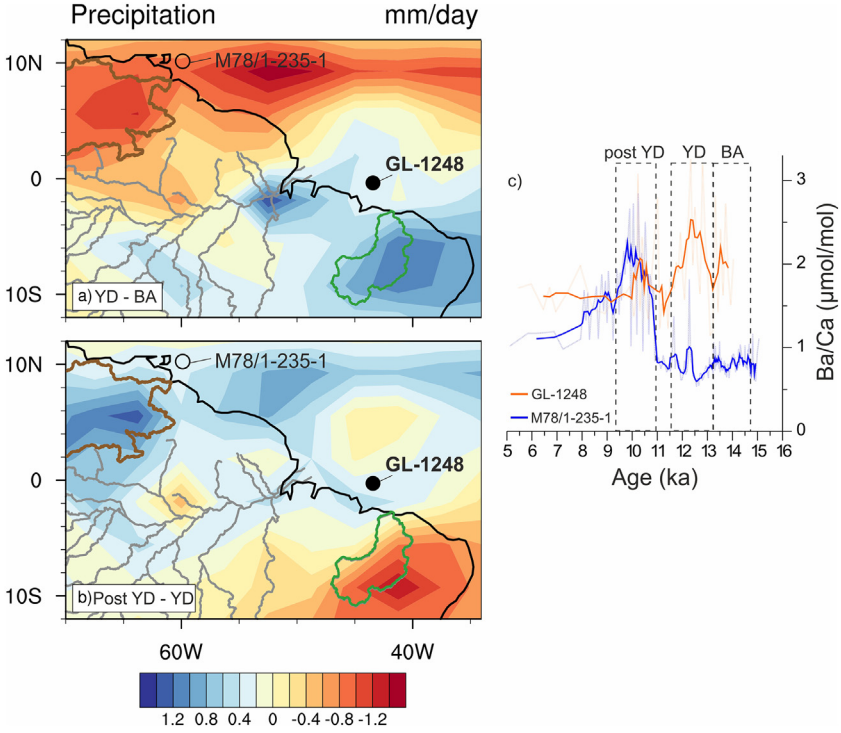

Fig. 3. Precipitation anomalies derived from TraCE-21 ka (Liu et al., 2009) results and Ba/Ca records from the western tropical Atlantic (Hoffmann et al., 2014; this study). (a) The panel shows the precipitation anomaly of the Younger Dryas relative to the Bølling–Allerød (YD-BA) and the location of cores GL-1248 and M78/1-235-1. (b) The panel shows the precipitation anomaly of a post-YD period (11–9.5 ka) relative to the YD (Post YD-YD) and the location of cores GL-1248 and M78/1-235-1. (c) The panel exhibits the Ba/Ca of *Globigerinoides ruber* from cores GL-1248 (this study; orange line) and M78/1-235-1 (Hoffmann et al., 2014; blue line). The dashed line bars mark the post-YD, YD and BA intervals. The thick lines in the right panels represent a 5-point running average. The lines in the continent represent the tributaries (or catchments) of the Amazon (grey), Parnaíba (green) and Orinoco Rivers (brown). (For interpretation of the references to color in this figure legend, the reader is referred to the web version of this article.)

our Ba/Ca results from core GL-1248 it is possible to capture the increase in river discharge to the ocean, which are probably related to the negative SSS anomaly close to the river mouths in the western equatorial Atlantic as indicated by TraCE-21 ka outputs (Fig. 1c), but not recorded by the $\delta^{18}O_{sw\text{-}ivc}$ from cores GL-1248 and GeoB16202-2 (Figs. 3).

During the YD, we observe high Ba/Ca values in core GL-1248 linked to enhanced fluvial discharge associated with a southern position of the ITCZ, while Ba/Ca record from core M78/1-235-1 (Hoffmann et al., 2014) exhibits low values during the same period (Fig. 3a). Afterwards, during the transition to the Holocene, Ba/Ca decreases for core GL-1248 but increases for core M78/1-235-1, and from 11 to 10 ka Ba/Ca values increases abruptly for core M78/1-235-1 and a minor increase is observed for GL-1248 (Fig. 3b). Hoffmann et al. (2014) argue that their high Ba/Ca values in the early Holocene indicate a change in the source of fluvial waters due to a northward shift of the ITCZ induced by increased low-latitude Northern Hemisphere summer insolation. A Ba/Ca record from the eastern tropical Atlantic further supports a southward shift of the ITCZ during the YD (MD03-2707; Weldeab et al., 2007). The comparison between the three available Ba/Ca records from the tropical Atlantic show decreased fluvial discharge from the Orinoco and Niger-Sanaga Rivers, while an increase in fluvial discharge is observed in the Parnaíba River (Fig. S9b). Results from the TraCE-21 ka support these findings, showing a decrease in precipitation in the Orinoco and Niger-Sanaga River basins and an increase in the Parnaíba River basin (Fig. S9a). Since fluvial discharge at these sites is influenced by continental precipitation changes linked to the ITCZ, it is possible to track the ITCZ position using the Ba/Ca records from these cores. Thus, the ITCZ reached its southernmost position between 13 and 11.8 ka, where Ba/Ca from core GL-1248 were maximum, and started to move northward reaching its northernmost position between 10.8 and 9.7 ka, where Ba/Ca from core M78/1–235-1 exhibit the highest values.

6. Conclusions

Paleoclimate records from the western tropical Atlantic were compared to TraCE-21 ka outputs and used to constrain the changes in surface hydrography during the YD. Proxy data and model results for the TSA agree well, showing ca. 1 °C warming during the YD relative to the BA (YD-BA). Such warming was probably the result of a weakening of the AMOC and of the western boundary currents. However, in the TNA the proxy and model results show disagreements. This is probably related to the competing atmospheric and oceanic mechanisms acting in this area during the YD, and/or to different proxy sensitivity. In the case of SSS changes, TraCE-21 ka outputs suggest a widespread decrease in SSS during the YD, which is not corroborated by the proxy ($\delta^{18}O_{sw\text{-}ivc}$) records. Such disagreement may be explained by (i) the fact that TraCE-21 ka do not appropriately simulate tropical salinity, and (ii) because of the opposite SSS anomalies triggered by a decrease in AMOC strength (positive) and by the enhanced continental freshwater discharge and direct precipitation (negative), which influences the $\delta^{18}O_{sw\text{-}ivc}$ records differently depending on their location. The Ba/Ca of *G. ruber* (white) from core GL-1248 reveals an increase in runoff during the YD, which is supported by high Fe/Ca values in the same core. Further, the comparison between the Ba/Ca records from cores GL-1248 and M78/1–235-1 indicates a southward (northward) displacement of the ITCZ during the YD (early Holocene). This highlights the potential of Ba/Ca records along the western tropical Atlantic to constrain past ITCZ shifts.

Acknowledgments, Samples, and Data

We thank R. Kowsman (CENPES/ Petrobras) and Petrobras Core Repository staff (Macaé/Petrobras) for providing the sediment core employed in this research. We thank S. Pape and M. Kölling for performing Mg/Ca analysis. CAPES financially supported I. M. V. with a scholarship (grant 88887.156152/2017-00 and 88881.161151/2017-01). T. P. S. acknowledges the financial support from CAPES/PDSE (grant 99999.007924/2014-03). A. L. A. is a CNPq senior researcher (grant 306385/2013-9) and thanks them for financial support (grant 99999.002675/2015-03). C. M. C. acknowledges the financial support from FAPESP (grant 2018/15123-4), CAPES (grant 564/2015), CNPq (grants 302607/2016-1 and 422255/2016-5) and the Alexander von Humboldt Foundation. This study was supported by CAPES-ASPECTO project (grant 88887.091731/2014-01). This work was also funded through the DFG Research Center/Cluster of Excellence "The Ocean in the Earth System" and by the Helmholtz Climate Initiative REKLIM. The data reported in this paper will be archived in Pangaea (www.pangaea.de).

Appendix A. Supplementary data

Supplementary data to this article can be found online at https://doi.org/10.1016/j.gloplacha.2019.103047.

References

Anand, P., Elderfield, H., Conte, M.H., 2003. Calibration of Mg/Ca thermometry in planktonic foraminifera from a sediment trap time series. Paleoceanography 18 (2). https://doi.org/10.1029/2002PA000846. n/a-n/a.

Arz, H.W., Pätzold, J., Wefer, G., 1999. The deglacial history of the western tropical Atlantic as inferred from high resolution stable isotope records off northeastern Brazil. Earth Planet. Sci. Lett. 167 (1–2), 105–117. https://doi.org/10.1016/S0012-821X(99)00025-4.

Bahr, A., Schönfeld, J., Hoffmann, J., Voigt, S., Aurahs, R., Kucera, M., ... Gerdes, A., 2013. Comparison of Ba/Ca and $\delta^{18}O_{WATER}$ as freshwater proxies: a multi-species core-top study on planktonic foraminifera from the vicinity of the Orinoco River mouth. Earth Planet. Sci. Lett. 383, 45–57. https://doi.org/10.1016/j.epsl.2013.09.036.

Bard, E., Rostek, F., Turon, J.L., Gendreau, S., 2000. Hydrological impact of Heinrich events in the subtropical Northeast Atlantic. Science 289 (5483), 1321–1324. https://doi.org/10.1126/science.289.5483.1321.

Barker, S., Greaves, M., Elderfield, H., 2003. A study of cleaning procedures used for foraminiferal Mg/Ca paleothermometry. Geochem. Geophys. Geosyst. 4 (9). https://doi.org/10.1029/2003GC000559.

Blaauw, M., 2010. Methods and code for "classical" age-modelling of radiocarbon sequences. Quat. Geochronol. 5 (5), 512–518. https://doi.org/10.1016/j.quageo.2010.01.002.

Blaauw, M., Christeny, J.A., 2011. Flexible paleoclimate age-depth models using an autoregressive gamma process. Bayesian Anal. 6 (3), 457–474. https://doi.org/10.1214/11-BA618.

Bouimetarhan, I., Chiessi, C.M., González-Arango, C., Dupont, L., Voigt, I., Prange, M., Zonneveld, K., 2018. Intermittent development of forest corridors in northeastern Brazil during the last deglaciation: Climatic and ecologic evidence. Quat. Sci. Rev. 192, 86–96. https://doi.org/10.1016/j.quascirev.2018.05.026.

Broecker, W.S., Peteet, D.M., Rind, D., 1985. Does the ocean-atmosphere system have more than one stable mode of operation? Nature 315 (6014), 21–26. https://doi.org/10.1038/315021a0.

Carlson, A.E., 2013. The Younger Dryas climate event. In: Encyclopedia of Quaternary Science: Second Edition, pp. 126–134. https://doi.org/10.1016/B978-0-444-53643-3.00029-7.

Chang, P., Ji, L., Li, H., 1997. A decadal climate variation in the tropical Atlantic Ocean from thermodynamic air-sea interactions. Nature 385 (6616), 516–518. https://doi.org/10.1038/385516a0.

Chang, P., Zhang, R., Hazeleger, W., Wen, C., Wan, X., Ji, L., ... Seidel, H., 2008. Oceanic link between abrupt changes in the North Atlantic Ocean and the African monsoon. Nat. Geosci. 1 (7), 444–448. https://doi.org/10.1038/ngeo218.

Chiang, J.C.H., Bitz, C.M., 2005. Influence of high latitude ice cover on the marine Intertropical Convergence Zone. Clim. Dyn. 25 (5), 477–496. https://doi.org/10.1007/s00382-005-0040-5.

Crivellari, S., Chiessi, C.M., Kuhnert, H., Häggi, C., Mollenhauer, G., Hefter, J., Mulitza, S., 2019. Thermal response of the western tropical Atlantic to slowdown of the Atlantic Meridional Overturning Circulation. Earth Planet. Sci. Lett. https://doi.org/10.1016/j.epsl.2019.05.006.

Firestone, R.B., West, A., Kennett, J.P., Becker, L., Bunch, T.E., Revay, Z.S., ... Wolbach, W.S., 2007. Evidence for an extraterrestrial impact 12,900 years ago that contributed to the megafaunal extinctions and the Younger Dryas cooling. Proc. Natl. Acad. Sci. 104 (41), 16016–16021. https://doi.org/10.1073/pnas.0706977104.

Grant, K.M., Rohling, E.J., Bar-Matthews, M., Ayalon, A., Medina-Elizalde, M., Ramsey, C.B., ... Roberts, A.P., 2012. Rapid coupling between ice volume and polar temperature over the past 150,000 years. Nature 491 (7426), 744–747. https://doi.org/10.1038/nature11593.

Groeneveld, J., Chiessi, C.M., 2011. Mg/Ca of Globorotalia inflata as a recorder of permanent thermocline temperatures in the South Atlantic. Paleoceanography 26 (2).

https://doi.org/10.1029/2010PA001940.
Guilderson, T.P., Fairbanks, R.G., Rubenstone, J.L., 2001. Tropical Atlantic coral oxygen isotopes: Glacial-interglacial Sea surface temperatures and climate change. Mar. Geol. 172 (1–2), 75–89. https://doi.org/10.1016/S0025-3227(00)00115-8.
Hall, J.M., Chan, L.-H., 2004. Ba/Ca in Neogloboquadrina pachyderma as an indicator of deglacial meltwater discharge into the western Arctic Ocean. Paleoceanography *19* (1). https://doi.org/10.1029/2003PA000910. n/a-n/a.
Hastenrath, S., Merle, J., 1987. Annual cycle of subsurface thermal structure in the tropical Atlantic Ocean. J. Phys. Oceanogr. 17 (9), 1518–1538. https://doi.org/10.1175/1520-0485(1987)017<1518:ACOSTS>2.0.CO;2.
Haug, G.H., Hughen, K.A., Sigman, D.M., Peterson, L.C., Röhl, U., 2001. Southward migration of the intertropical convergence zone through the Holocene. Science 293 (5533), 1304–1308. https://doi.org/10.1126/science.1059725.
He, F., 2011. Simulating transient climate evolution of the last deglaciation with CCSM3. In: Ph.D Thesis. Department of Atmospheric and Oceanic Sciences, University of Wisconsin-Madison, pp. 161.
Hoffmann, J., Bahr, A., Voigt, S., Schönfeld, J., Nürnberg, D., Rethemeyer, J., 2014. Disentangling abrupt deglacial hydrological changes in northern South America: insolation versus oceanic forcing. Geology 42 (7), 579–582. https://doi.org/10.1130/G35562.1.
Hönisch, B., Allen, K.A., Russell, A.D., Eggins, S.M., Bijma, J., Spero, H.J., ... Yu, J., 2011. Planktic foraminifers as recorders of seawater Ba/Ca. Mar. Micropaleontol. 79 (1–2), 52–57. https://doi.org/10.1016/j.marmicro.2011.01.003.
Hut, G., 1987. Stable isotope reference samples for geochemical and hydrological investigations. In: Report of Consultant's Group Meeting. International Atomic Energy Agency, Vienna, Austria, pp. 42.
Jaeschke, A., Rühlemann, C., Arz, H., Heil, G., Lohmann, G., 2007. Coupling of millennial-scale changes in sea surface temperature and precipitation off northeastern Brazil with high-latitude climate shifts during the last glacial period. Paleoceanography 22 (4). https://doi.org/10.1029/2006PA001391.
Johnson, R.G., McClure, B.T., 1976. A model for Northern Hemisphere continental ice sheet variation. Quat. Res. 6 (3), 325–353. https://doi.org/10.1016/0033-5894(67)90001-4.
Kageyama, M., Mignot, J., Swingedouw, D., Marzin, C., Alkama, R., Marti, O., 2009. Glacial climate sensitivity to different states of the Atlantic meridional overturning circulation: results from the IPSL model. Clim. Past 5 (3), 551–570. https://doi.org/10.5194/cp-5-551-2009.
Knutti, R., Flückiger, J., Stocker, T.F., Timmermann, A., 2004. Strong hemispheric coupling of glacial climate through freshwater discharge and ocean circulation. Nature. https://doi.org/10.1038/nature02786.
Lea, D.W., Pak, D.K., Peterson, L.C., Hughen, K.A., 2003. Synchroneity of tropical and high-latitude Atlantic temperatures over the last glacial termination. Science 301 (5638), 1361–1364. https://doi.org/10.1126/science.1088470.
Liu, Z., Otto-Bliesner, B.L., He, F., C, E., Brady, R.T., Clark, P.U., Carlson, A.E., ... Tomas, R., 2009. Transient simulation of last deglaciation with a new mechanism for Bølling-Allerød warming. Science 325 (5938), 310–314. https://doi.org/10.1126/science.1171041.
Mahajan, S., Saravanan, R., Chang, P., 2011. The role of the wind-evaporation-sea surface temperature (WES) feedback as a thermodynamic pathway for the equatorward propagation of high-latitude sea ice-induced cold anomalies. J. Clim. 24 (5), 1350–1361. https://doi.org/10.1175/2010JCLI3455.1.
McManus, J.F., Francois, R., Gherardl, J.M., Kelgwin, L., Drown-Leger, S., 2004. Collapse and rapid resumption of Atlantic meridional circulation linked to deglacial climate changes. Nature 428 (6985), 834–837. https://doi.org/10.1038/nature02494.
Mulitza, S., Boltovskoy, D., Donner, B., Meggers, H., Paul, A., Wefer, G., 2003. Temperature: δ18O relationships of planktonic foraminifera collected from surface waters. Palaeogeogr. Palaeoclimatol. Palaeoecol. 202 (1–2), 143–152. https://doi.org/10.1016/S0031-0182(03)00633-3.
Mulitza, S., Chiessi, C.M., Schefuß, E., Lippold, J., Wichmann, D., Antz, B., ... Zhang, Y., 2017. Synchronous and proportional deglacial changes in Atlantic meridional overturning and northeast Brazilian precipitation. Paleoceanography 32 (6), 622–633. https://doi.org/10.1002/2017PA003084.
Muller-Karger, F.E., McClain, C.R., Richardson, P.L., 1988. The dispersal of the Amazon's water. Nature 333 (6168), 56–59. https://doi.org/10.1038/333056a0.
Nace, T.E., Baker, P.A., Dwyer, G.S., Silva, C.G., Rigsby, C.A., Burns, S.J., ... Zhu, J., 2014. The role of North Brazil current transport in the paleoclimate of the Brazilian Nordeste margin and paleoceanography of the western tropical Atlantic during the late Quaternary. Palaeogeogr. Palaeoclimatol. Palaeoecol. 415, 3–13. https://doi.org/10.1016/j.palaeo.2014.05.030.
North Greenland Ice Core Project members, 2004. High-resolution record of Northern Hemisphere climate extending into the last interglacial period. Nature 431 (7005), 147–151. https://doi.org/10.1038/nature02805.
Peterson, R.G., Stramma, L., 1991. Upper-level circulation in the South Atlantic Ocean. Prog. Oceanogr. https://doi.org/10.1016/0079-6611(91)90006-8.
Portilho-Ramos, R.C., Chiessi, C.M., Zhang, Y., Mulitza, S., Kucera, M., Siccha, M., ... Paul, A., 2017. Coupling of equatorial Atlantic surface stratification to glacial shifts in the tropical rainbelt. Sci. Rep. 7 (1). https://doi.org/10.1038/s41598-017-01629-z.
Rama-Corredor, O., Martrat, B., Grimalt, J.O., López-Otalvaro, G.E., Flores, J.A., Sierro, F., 2015. Parallelisms between sea-surface temperature changes in the western tropical Atlantic (Guiana Basin) and high latitude climate signals over the last 140 000 years. Clim. Past 11 (10), 1297. Retrieved from. http://www.clim-past.net/11/1297/2015/cp-11-1297-2015.pdf.
Reimer, P.J., Bard, E., Bayliss, A., Beck, J.W., Blackwell, P.G., Bronk, M., ... van der Plicht, J., 2013. IntCal 13 and Marine 13 radiocarbon age calibration curves 0–50,000 years cal BP. Radiocarbon 55, 1869–1887. https://doi.org/10.2458/azu.
Reißig, S., Nürnberg, D., Bahr, A., Poggemann, D.W., Hoffmann, J., 2019. Southward displacement of the North Atlantic subtropical gyre circulation system during North Atlantic cold spells. Paleoceanogr. Paleoclimatol. https://doi.org/10.1029/2018PA003376.
Renssen, H., Van Geel, B., Van Der Plicht, J., Magny, M., 2000. Reduced solar activity as a trigger for the start of the Younger Dryas? Quat. Int. 68–71, 373–383. https://doi.org/10.1016/S1040-6182(00)00060-4.
Renssen, H., Mairesse, A., Goosse, H., Mathiot, P., Heiri, O., Roche, D.M., ... Valdes, P.J., 2015. Multiple causes of the Younger Dryas cold period. Nat. Geosci. 8 (12), 946–949. https://doi.org/10.1038/ngeo2557.
Rodrigues, R.R., Rothstein, L.M., Wimbush, M., 2007. Seasonal variability of the South Equatorial Current bifurcation in the Atlantic Ocean: A numerical study. Journal of Physical Oceanography. https://doi.org/10.1175/JPO2983.1.
Rooth, C., 1982. Hydrology and ocean circulation. Prog. Oceanogr. 11 (2), 131–149. https://doi.org/10.1016/0079-6611(82)90006-4.
Rühlemann, C., Mulitza, S., Müller, P.J., Wefer, G., Zahn, R., 1999. Warming of the tropical Atlantic Ocean and slowdown of thermohaline circulation during the last deglaciation. Nature 402 (6761), 511–514. https://doi.org/10.1038/990069.
Schmidt, M.W., Spero, H.J., Lea, D.W., 2004. Links between salinity variation in the Caribbean and North Atlantic thermohaline circulation. Nature 428 (6979), 160–163. https://doi.org/10.1038/nature02346.
Schmidt, M.W., Chang, P., Hertzberg, J.E., Them, T.R., Ji, L., Otto-Bliesner, B.L., 2012. Impact of abrupt deglacial climate change on tropical Atlantic subsurface temperatures. Proc. Natl. Acad. Sci. 109 (36), 14348–14352. https://doi.org/10.1073/pnas.1207806109.
Schrag, D.P., Adkins, J.F., McIntyre, K., Alexander, J.L., Hodell, D.A., Charles, C.D., McManus, J.F., 2002. The oxygen isotopic composition of seawater during the last glacial maximum. Quat. Sci. Rev. 21 (1–3), 331–342. https://doi.org/10.1016/S0277-3791(01)00110-X.
Shakun, J.D., Clark, P.U., He, F., Marcott, S.A., Mix, A.C., Liu, Z., ... Bard, E., 2012. Global warming preceded by increasing carbon dioxide concentrations during the last deglaciation. Nature 484 (7392), 49–54. https://doi.org/10.1038/nature10915.
Stramma, L., England, M., 1999. On the water masses and mean circulation of the South Atlantic Ocean. J. Geophys. Res Oceans 104 (C9), 20863–20883. https://doi.org/10.1029/1999JC900139.
Stramma, L., Fischer, J., Reppin, J., 1995. The North Brazil Undercurrent. Deep-Sea Res. I 42 (5), 773–795. https://doi.org/10.1016/0967-0637(95)00014-W.
Vahlenkamp, M., 2013. The anatomy of heinrich event 1 – a multiproxy study of centennial to millennial scale climate change off Brazil. In: Master's Thesis. University of Bremen, pp. 70.
Venancio, I.M., Mulitza, S., Govin, A., Santos, T.P., Lessa, D.O., Albuquerque, A.L.S., Chiessi, C.M., Tiedemann, R., Vahlenkamp, M., Bickert, T., Schulz, M., 2018. Millennial- to orbital-scale responses of western equatorial Atlantic thermocline depth to changes in the trade wind system since the last Interglacial. Paleoceanogr. Paleoclimatol. 33, 1490–1507. https://doi.org/10.1029/2018PA003437.
Wan, X., Chang, P., Saravanan, R., Zhang, R., Schmidt, M.W., 2009. On the interpretation of Caribbean paleo-temperature reconstructions during the Younger Dryas. Geophys. Res. Lett. 36 (2). https://doi.org/10.1029/2008GL035805.
Wan, X., Chang, P., Schmidt, M.W., 2010. Causes of tropical Atlantic paleo-salinity variation during periods of reduced AMOC. Geophys. Res. Lett. 37 (4). https://doi.org/10.1029/2009GL042013.
Wang, X., Auler, A.S., Edwards, L.L., Cheng, H., Cristalli, P.S., Smart, P.L., ... Shen, C.C., 2004. Wet periods in northeastern Brazil over the past 210 kyr linked to distant climate anomalies. Nature 432 (7018), 740–743. https://doi.org/10.1038/nature03067.
Weldeab, S., Schneider, R.R., Kölling, M., 2006. Deglacial sea surface temperature and salinity increase in the western tropical Atlantic in synchrony with high latitude climate instabilities. Earth Planet. Sci. Lett. 241 (3–4), 699–706. https://doi.org/10.1016/j.epsl.2005.11.012.
Weldeab, S., Lea, D.W., Schneider, R.R., Andersen, N., 2007. 155,000 years of West African monsoon and ocean thermal evolution. Science 316 (5829), 1303–1307. https://doi.org/10.1126/science.1140461.
Xie, S., Philander, S.G.H., 1994. A coupled ocean-atmosphere model of relevance to the ITCZ in the eastern Pacific. *Tellus* A 46 (4), 340–350. https://doi.org/10.1034/j.1600-0870.1994.t01-1-00001.x.
Zhang, Y., Chiessi, C.M., Mulitza, S., Zabel, M., Trindade, R.I.F., Hollanda, M.H.B.M., ... Wefer, G., 2015. Origin of increased terrigenous supply to the NE South American continental margin during Heinrich Stadial 1 and the Younger Dryas. Earth Planet. Sci. Lett. 432, 493–500. https://doi.org/10.1016/j.epsl.2015.09.054.